Published in final edited form as:
Cell. 2014 December 4; 159(6): 1341–1351. doi:10.1016/j.cell.2014.10.049.

Species-wide Genetic Incompatibility Analysis Identifies Immune Genes as Hotspots of Deleterious Epistasis

Eunyoung Chae[1], **Kirsten Bomblies**[1,†], **Sang-Tae Kim**[1], **Darya Karelina**[1,2], **Maricris Zaidem**[1], **Stephan Ossowski**[1,†], **Carmen Martín-Pizarro**[1], **Roosa A. E. Laitinen**[1,†], **Beth A. Rowan**[1], **Hezi Tenenboim**[1,†], **Sarah Lechner**[1,†], **Monika Demar**[1], **Anette Habring-Müller**[1], **Christa Lanz**[1], **Gunnar Rätsch**[2,†], and **Detlef Weigel**[1,*]

[1]Department of Molecular Biology, Max Planck Institute for Developmental Biology, 72076 Tübingen, Germany

[2]Friedrich Miescher Laboratory of the Max Planck Society, 72076 Tübingen, Germany

Summary

Intraspecific genetic incompatibilities prevent the assembly of specific alleles into single genotypes and influence genome- and species-wide patterns of sequence variation. A common incompatibility in plants is hybrid necrosis, characterized by autoimmune responses due to epistatic interactions between natural genetic variants. By systematically testing thousands of F_1 hybrids of *Arabidopsis thaliana* strains, we identified a small number of incompatibility hotspots in the genome, often in regions densely populated by NLR immune receptor genes. In several cases, these immune receptor loci interact with each other, suggestive of conflict within the immune system. A particularly dangerous locus is a highly variable cluster of NLR genes, *DANGEROUS MIX2* (*DM2*), which causes multiple, independent incompatibilities with genes that encode a range of biochemical functions, including NLRs. Our findings suggest that deleterious interactions of immune receptors at the front lines of host-pathogen co-evolution limit the combinations of favorable disease resistance alleles accessible to plant genomes.

Keywords

hybrid incompatibility; hybrid necrosis; epistasis; autoimmunity; NLR; *Arabidopsis thaliana*

*Corresponding author; weigel@weigelworld.org.
†Current addresses: Department of Organismic and Evolutionary Biology, Harvard University, Cambridge, Massachusetts 02138, USA (K.B.); Center for Genomic Regulation and Universitat Pompeu Fabra, 08003 Barcelona, Spain (S.O.); Max Planck Institute of Molecular Plant Physiology, 14476 Potsdam-Golm, Germany (R.A.L.; H.T.); CeGAT GmbH, 72076 Tübingen, Germany (S.L.); Memorial Sloan-Kettering Cancer Center, New York City, New York 10065, USA (G.R.)

Author Contributions

Conceived and designed the experiments: E.C., K.B. and D.W. Performed the experiments: E.C., K.B., S.-T. K., M.Z., C.M.P., H.T., S.L., A.H.-M., M.D., C.L. Analyzed the data: E.C., K.B., S.-T. K., D.K., M.Z., S.O., R.A.L., B.A.R., G.R. Wrote the paper: E.C., K.B. and D.W. with contributions from all authors.

Introduction

When independently diverging genomes meet in hybrids, the differences that have accumulated over evolutionary time can have detrimental consequences. The ensuing incompatibilities were formally described by Bateson, Dobzhansky and Muller, who proposed a scenario under which complementary changes occur in two different populations; the individual changes are innocuous in their native genomic contexts, and they reduce viability or fertility only when combined in hybrids (Coyne and Orr, 2004). This type of deleterious, or negative, epistasis has been most prominently studied in interspecific crosses, where the interacting alleles are fixed in the different populations (Maheshwari and Barbash, 2011; Presgraves, 2010; Rieseberg and Blackman, 2010). More recent work has begun to focus on deleterious epistasis within species, where the interacting alleles are polymorphic and segregate in a single intermating population (Corbett-Detig et al., 2013; Hou et al., 2014; Seidel et al., 2008). One can envision a series of evolutionary forces responsible for the emergence of interacting alleles. On the one hand, genetic drift could play a role, with segregating alleles that are neutral or merely mildly deleterious on their own giving rise to synthetic deleterious interactions (Bikard et al., 2009; Phillips and Johnson, 1998). At the other end of the spectrum, adaptation and intragenomic conflicts have been implicated as factors that may contribute to a reduction in hybrid viability or fertility (Crespi and Nosil, 2013; Cutter, 2012; Lachance and True, 2010). Regardless of the ultimate cause, high levels of sequence divergence at incompatibility loci appear to be positively correlated with deleterious interactions. Ultimately, as lineages diverge and become genetically more differentiated, segregating variants may rise to high frequency in specific populations and thereby reduce gene flow among them.

Genes of the immune system are particularly polymorphic in many organisms, because of an evolutionary arms race between hosts and pathogens (Quintana-Murci and Clark, 2013; Sackton et al., 2007; Vilches and Parham, 2002). This is also true for plants. Prominent, highly variable components of the plant immune system are the nucleotide-binding domain and leucine-rich repeat (NLR) proteins, with plant genomes often encoding hundreds of NLRs (Cao et al., 2011; Jacob et al., 2013). Plant NLRs typically function as immune receptors that confer disease resistance by monitoring the integrity of important plant proteins or the presence of pathogen effector proteins (Collier and Moffett, 2009).

Apart from having to keep up with the ongoing evolution of individual pathogens, hosts must also accumulate resistance against as many different pathogens as possible. This in turn entails its own dangers, in the form of genetic variants that lead to enhanced immunity, but at the same time reduce growth or health due to autoimmunity (Todesco et al., 2010; Trowsdale and Knight, 2013). In plants, especially severe autoimmune phenotypes have been observed in hybrids descended from phenotypically normal parents. This syndrome, hybrid necrosis, is found in intra- and interspecific crosses and it spans a range of severity, from cases where only a small subset of F_2 progeny is weakly affected to ones in which all F_1 hybrids die. The lesions and reduced growth of necrotic hybrids are often alleviated at higher temperature, greatly facilitating the genetic analysis of severe cases (Bomblies and Weigel, 2007).

To date, four hybrid necrosis cases due to two-locus epistasis have been studied at the molecular level in tomato, lettuce and rice. Of the six causal loci that have been positively identified, one encodes an NLR and another one a known NLR-interactor. In addition, the mapping interval for one of the remaining loci includes several NLRs (Chen et al., 2014; Jeuken et al., 2009; Krüger et al., 2002; Yamamoto et al., 2010). Similarly, the first hybrid necrosis gene positively identified in *Arabidopsis thaliana*, *DANGEROUS MIX1* (*DM1*), encodes an NLR. It interacts with the *DM2* locus, which was mapped to a polymorphic cluster of *RPP1* NLR genes that is probably also responsible for an independent F_2 incompatibility (Alcázar et al., 2009; Bomblies et al., 2007). In natural accessions of *A. thaliana*, the *RPP*-subfamily of NLR genes is particularly variable, both in sequence and copy number. The high diversity of *RPP* loci, which recognize different strains of the oomycete pathogen *Hyaloperonospora arabidopsidis* ex *parasitica* (*Hpa*) in an allele-specific manner, points to these genes as actors in an active co-evolutionary tug-of-war between host and pathogen (Allen et al., 2004; Bakker et al., 2006; Holub and Beynon, 1997).

While there is increasing evidence for natural variation in immunity potentially leading to genetic incompatibilities in plants, species-wide patterns of immune-related deleterious epistasis remain unknown. For example, are specific immune loci especially likely to be involved in deleterious epistasis? Do they interact more often with other immune loci than with non-immune genes? And is deleterious epistasis correlated with geographic and genetic distance? To systematically investigate which factors in the plant immune system contribute to intraspecific incompatibility, we have examined F_1 progeny from thousands of *A. thaliana* crosses, including all combinations among 80 accessions that represent much of the common genetic diversity in the species (Cao et al., 2011). We have mapped several hybrid necrosis loci to regions of the genome that contain multiple NLR genes in tandem arrays, with different allelic variants at *DM2*/*RPP1* being responsible for several independent incompatibilities. We also found cases where different alleles at a locus interact with each other, or where independent pairs of alleles at two loci are incompatible with each other. Because many interactions are between components of the plant immune system, we propose that epistatic fitness effects limit the extent to which favorable immune alleles can be combined.

Results

A systematic resource for the discovery of genetic incompatibilities

About two percent of crosses between randomly chosen accessions of *A. thaliana* suffer from F_1 hybrid necrosis when grown at 16°C (Bomblies et al., 2007). To determine the incidence of hybrid necrosis and other F_1 weakness syndromes more systematically, and to obtain insights into how genetic kinship affects the probability of hybrid necrosis, we turned to 80 accessions that had their genomes sequenced in the first phase of the 1001 Genomes project (Cao et al., 2011). These 80 accessions represent much of the common diversity across the species' native range, and can thus provide insights into the distribution of hybrid necrosis alleles in both the global and in local populations. To facilitate the large number of crosses, male-sterile lines were derived by knocking down the floral homeotic gene *AP3*

(Wuest et al., 2012). Together with additional crosses that mostly involved accessions carrying known *DM* alleles, we assembled a total of 6,409 crosses. This collection comprised 3,330 unique parental combinations; 3,160 of these made up a complete half-diallel of the 80 accessions (Table S1).

The most common morphological defects seen in F_1 hybrids at 16°C were dwarfism and tissue necrosis, which fell into five classes of increasing severity, including two new extreme classes (Figures 1 and S1). In the previously described cases, morphological defects largely disappeared at 23°C (Bomblies et al., 2007). Class 4 phenotypes were only suppressed at 28°C, while class 5 individuals died as seedlings at all temperatures tested. Most necrotic hybrids had only mild defects (103 cases in class 1), 29 cases were intermediate (classes 2 to 4), and 10 cases were not genetically tractable due to lethality (class 5). Our threshold for identifying necrosis was quite stringent, and there might well be many more weak cases.

Mapping and identification of incompatibility loci

From the 142 F_1 hybrid necrosis cases described here and the 27 identified previously (Bomblies et al., 2007), we chose seven for further genetic analysis. In addition to obvious phenotypes, we prioritized cases where at least one of the causal alleles was likely to be present in multiple genetic backgrounds, as judged by one parent producing similar F_1 phenotypes with several other parents. Thus, the selected cases are likely to represent 31 of the 48 intermediate, genetically tractable hybrid necrosis examples in our collection.

The fraction of affected individuals in F_2 populations indicated that hybrid phenotypes in five cases were due to pairwise interactions between genetically separable loci (Table S2). Segregation ratios in Ey1.5-2 x ICE228 and for the Bla-1 x Hh-0 lesioning trait were consistent with effects arising from heterozygous disadvantage at single regions of the genome (Table S2). We mapped causal loci mostly using Genotyping-By-Sequencing (GBS) of individual F_2 plants (Elshire et al., 2011; Poland et al., 2012) and quantitative trait locus (QTL) methods (Table S3; Figures 2A–H). For leaf-twisting in Bla-1 x Hh-0, we used whole-genome sequencing of pooled DNA from F_1-like individuals segregating in selfed BC_5 progeny (Figures 2A, 2D and S2B).

Our analyses identified seven new hybrid necrosis loci, *DM3* to *DM9* (Figures 2 and S2A; Table 1), with final mapping intervals between 110 and 969 kb (Table S4). The *DM2* region was represented in multiple crosses: *DM3*, *DM4*, and *DM5* all interacted with *DM2* alleles from different strains, as do the previously identified *DM1* and *SRF3* loci (Alcázar et al., 2010; Bomblies et al., 2007). Thus, at least five out of nine *A. thaliana* hybrid necrosis cases include *DM2* as one of the interactors. Two cases mapped to different pairs of *DM6* and *DM7* alleles, and two involved heterozygous effects at single loci, *DM8* and *DM9*.

We identified the DM3 prolyl aminopeptidase (At3g61540) from Hh-0 as an interactor of DM2h from Bla-1 using transformation with genomic fragments and artificial miRNA (amiRNA) knockdown (Table 1; Figures 2 and S2B–E). In two crosses, KZ10 x Mrk-0 and Fei-0 x Lerik1-3, one of the causal loci, *DM7*, mapped to the *RESISTANCE TO POWDERY MILDEW8* (*RPW8*) region, which contains a variable tandem array of genes encoding

coiled-coil proteins (Xiao et al., 2001). Transgenic experiments revealed that *RPW8.1*^{KZ10} was sufficient to induce necrosis in the Mrk-0 background (Table 1; Figures 2 and S2F–G). Despite similar genomic locations of the incompatibility genes, KZ10 is compatible with Lerik1-3, and Mrk-0 with Fei-0 (Table S1), indicating that these incompatibilities likely include different pairs of alleles at *DM6* and *DM7*.

We mapped the *DM9* locus in two crosses, Bla-1 x Hh-0 (this work) and Mir-0 x Se-0. A detailed analysis of the causal locus, *ACCELERATED CELL DEATH6* (*ACD6*, is reported elsewhere (Todesco et al., 2014).

We confirmed genes from the *RPP7* and *RPP4/5* NLR clusters as causal for *DM6* and *DM8* using amiRNAs (Table 1). *DM4* also overlapped the location of an *RPP* cluster, *RPP8* (Table S4). Four out of nine *DM* loci, accounting for ten of the causal alleles, thus map to highly variable *RPP* clusters (Figure 2I), which are the major sources for resistance to *Hpa* in *A. thaliana* (Nemri et al., 2010). In one *DM2* case, discussed in detail below, we have direct evidence for interactions between two different NLR genes. Three other interactions, *DM2*/*DM4*, *DM2*/*DM5*, and the *DM8* heterozygous incompatibility, also likely involve interactions between NLR genes, while the *DM6/DM7* interactions involve an NLR candidate and a complex non-NLR immune locus, *RPW8* (Xiao et al., 2001). Finally, the heterozygous interaction at *DM9* is caused by distinct alleles of another complex non-NLR immune locus *ACD6* (Lu et al., 2003). Our systematic mapping efforts therefore indicate that NLR alleles along with other polymorphic immune genes located in tandem arrays are responsible for most intraspecific F_1 incompatibilities in *A. thaliana*.

Multiple incompatibilities due to the complex *RPP1*/*DM2* NLR locus

To understand how incompatibilities at *RPP* clusters evolve, we studied the *RPP1/DM2* locus from the accessions Uk-1 and Bla-1 in detail. We first assembled genomic sequences of the Uk-1 and Bla-1 *DM2* clusters from overlapping fosmid clones, and compared these with sequences from the L*er* and Col-0 accessions and the related species *A. lyrata*. In the *A. thaliana* reference strain Col-0, the *DM2* locus contains two *RPP1* paralogs that span 31 kb and that are part of a 180-kb *RPP1* supercluster. The *DM2* regions are much larger in Bla-1 and Uk-1, 119 kb and 128 kb (Figures 3A and S3). Both accessions contain eight *RPP1* paralogs, similar to the 92-kb *DM2*^{Ler} cluster, which includes seven complete and at least one truncated *RPP1* homolog (Alcázar et al., 2009). Not a single *RPP1-like* gene is identical between accessions, consistent with the pattern of accession-specific incompatibilities (Figure 3B).

To test which of the *RPP1*-like genes in Uk-1 and Bla-1 are responsible for hybrid necrosis, we first knocked down individual *DM2* genes with allele-specific amiRNAs (Figure S4A and Supplemental Experimental Procedures). We also introduced *DM2* genomic clones into the incompatible parents Uk-3, which carries a *DM2* interactor at *DM1*, and Hh-0, which carries a *DM2* interactor at *DM3* (Table 1). These experiments identified single genes in each accession, *DM2d*$^{Uk-1}$ and *DM2h*$^{Bla-1}$, as necessary and sufficient for hybrid necrosis (Figures 4A and S4B–G).

We asked whether autoimmunity depended on additional factors specific to the incompatible accessions. We first reconstituted the *DM2*$^{Uk-1}$/*DM1*$^{Uk-3}$ and *DM2*$^{Bla-1}$/*DM3*$^{Hh-0}$ interactions in the Col-0 background by crossing lines with the respective transgenes; in both cases doubly transgenic lines were severely necrotic (Figure 4B). Next, we transiently expressed each pair in *Nicotiana benthamiana* leaves. We observed necrosis symptoms that mimicked the hypersensitive response (HR) seen upon recognition of a pathogen by a plant host when incompatible alleles of *DM2* and *DM1*, or *DM2* and *DM3* were combined (Figure 4C). Importantly, *DM2* genes closely related to either *DM2d*$^{Uk-1}$ or *DM2h*$^{Bla-1}$ did not trigger HR-like necrosis in *N. benthamiana* when combined with *DM1*$^{Uk-3}$ or *DM3*$^{Hh-0}$ (Figure 4C), confirming that HR is not simply induced by any combination of foreign NLR genes. Furthermore, enzymatic activity of DM2 was required for HR in this system (Figure 4C), indicating that DM2 directly couples to downstream signaling events (Chung et al., 2011). These results demonstrate that incompatible pairs of DM proteins are sufficient to initiate cell death signaling conserved between species.

Distinct evolutionary histories of two causal *DM2* alleles

Not all clades in a *DM2* phylogeny (Figures S4H–J) include *DM2* genes from all accessions. In addition, relationships among accessions within one clade often differ from those in another clade. Thus, likely as a result of independent cycles of local gene duplication and loss along with illegitimate recombination and gene conversion (Table S5), *DM2* clusters from different lineages show little conserved synteny, vary in size, and are poorly conserved outside NLR gene fragments (Figure 3A). This is consistent with patterns reported for major immune receptor gene clusters throughout flowering plants (Jacob et al., 2013).

Despite the overall similarity of *DM2h*/*At3g44670* alleles among several accessions (Figure S4H–J), the LRR region, which is likely responsible for pathogen recognition, showed signs of diversifying selection (Figures 5A and S5A–B; average $K_a/K_s = 4.2$ for codons encoding the putative solvent-exposed residues). We thus hypothesized that rare allelic differences in a rapidly evolving portion of this gene gave rise to the incompatible behavior of *DM2h*$^{Bla-1}$. We localized residues responsible for incompatibility with *DM3* using domain swaps. We first mapped the incompatible sequences to the C-terminus of the DM2h^{Bla-1} protein, which includes the LRRs (Figure S5C). By engineering polymorphisms from *DM2h*$^{Bla-1}$ that are rare in other accessions into the *At3g44670*$^{Col-0}$ reference allele (Figures S5A and S5B), we identified two adjacent residues in the putative solvent exposed site of LRR4 that can confer partial necrosis-inducing activity when combined with C-terminal sequences (Figure S5D). This result highlights the potential of natural NLR variants for the identification of residues that increase protein activity, which would inform efforts to engineer semi-synthetic NLRs (Harris et al., 2013; Segretin et al., 2014).

RPP1-type proteins recognize and associate with proteins encoded by the *Hpa* ATR effector locus in an allele-specific manner (Krasileva et al., 2010). The hybrid necrosis-inducing residues in *DM2h*$^{Bla-1}$ mapped near a modeled docking site of ATR1 onto RPP1-WsB (Steinbrenner et al., 2012), suggesting that these variants have arisen from an arms-race between an immune receptor and a pathogen ligand.

The topology of genes in the *DM2*$^{Uk\text{-}1}$ cluster, as well as the phylogenetic relationships between *DM2* genes, suggested that *DM2d*$^{Uk\text{-}1}$ arose by two within-cluster duplications and involved at least three gene conversion events (Figure 5B; Table S5). The two closest paralogs within the Uk-1 cluster are *DM2e* and *DM2g*, with *DM2e* having suffered mutations that truncate the encoded protein (Figures 5B, S3 and S4H–J). Despite being within-cluster duplicates, *DM2d*$^{Uk\text{-}1}$ and *DM2g*$^{Uk\text{-}1}$ differ at many non-synonymous sites, partly due to sequence exchanges with different paralogs (Figure 5A; Table S5). We visualized broader patterns of variation by using *DM2d*$^{Uk\text{-}1}$ as a target for mapping of Illumina reads from 87 accessions. Accessions with very similar sequences across the entire gene were rare (Figure 5D). Moreover, similarity did not predict incompatibility: although ICE97 from Southern Italy has a *DM2d* copy that is very similar to that of Uk-1, ICE97 was not incompatible with Uk-3 (Table S1). The rarity of *DM2d*$^{Uk\text{-}1}$ is consistent with the hypothesis that *DM2d* is a rapidly evolving type I plant NLR gene, characterized by frequent sequence exchanges with other members of the same cluster (Kuang et al., 2004).

Unlike *DM2d*$^{Uk\text{-}1}$, *DM2h*$^{Bla\text{-}1}$ shows a clear orthologous relationship with *DM2* genes in other accessions, *At3g44670*$^{Col\text{-}0}$ and *At3g44670*^{Ler} (Figures 5C and S4H–J), a pattern typical for type II plant NLR genes (Kuang et al., 2004). Alleles at type II genes, which can be rare or common, diversify mostly by point mutations in the LRR region, rather than by sequence exchanges between paralogs. All three *DM2h*-type orthologs, *DM2h*$^{Bla\text{-}1}$, *At3g44670*$^{Col\text{-}0}$ and *At3g44670*^{Ler}, are located at the 3′ end of the *DM2* cluster and mark the beginning of a syntenic region of at least 22 kb that is well conserved between L*er*, Col-0 and Bla-1, but that is not found in Uk-1 or *A. lyrata* (Figures 3A and 6A). *DM2* hybrid necrosis alleles thus have arisen both as diversified orthologs and as paralogs within the tandemly arrayed gene cluster, accompanied by diversifying selection.

To assess the prevalence of haplotype sharing in this region, we asked whether the 3′ syntenic region is present in 16 additional accessions with a *DM2h*-type gene (Figure 5D; Table S6). Reconstruction of phylogenetic relationships across an 8 kb region demonstrated that at least 12 of the *DM2h* carriers shared very similar sequences in this region (Figure 6B). Close relationships were not evident on the other side of the *DM2* cluster (Figure S6A), arguing against reduced haplotype diversity being simply a consequence of suppressed recombination, as reported for some NLR clusters (Chin et al., 2001). Such haplotype sharing among the 12 carriers, which extended over a region of 16 kb downstream of *DM2h*/*At3g44670* (Welch two sample *t*-test, $P<0.0001$), was not observed next to two other NLR loci, the *RPM1* single-gene locus and the *RPP4/5* cluster (Figure 6C). We further confirmed haplotype sharing at *DM2* among the *DM2h* carriers using the F_{ST} statistic as a proxy for genetic differentiation (Figure S6B). Together with the observation that the 12 accessions are otherwise not particularly related either (Figure 6D), this suggests that the pattern of reduced haplotype diversity is not due to a recent population bottleneck.

Geographic distribution of hybrid necrosis risk alleles

Two proteins that can produce hybrid necrosis in combination with *DM2* alleles from Uk-3 and L*er* have been previously identified, the NLR protein DM1 from Uk-1 (Bomblies et al., 2007) and the kinase SRF3 from Central Asian accessions (Alcázar et al., 2010). In this

study, we identified the prolyl aminopeptidase DM3 from Hh-0 as an interactor of DM2h from Bla-1 (Figures 6E and S2B–E). In addition, the *DM2* cluster from Dog-4 interacts with an unknown gene at the *DM5* locus from ICE163, while the *DM2* clusters from several South Tyrolean accessions including ICE163 interact with *DM4* from TueWa1-2 (Figure 6E). We analyzed the genome-wide differentiation of *DM2* risk allele carriers among the 80 accessions that served as parents of many of our hybrid crosses plus other known carriers. As expected, accessions with different *DM2* alleles did not cluster with each other, but rather with other accessions from the same geographical regions (Figure 6D), supporting independent origins of the different risk alleles. One of the *DM2* risk alleles was present in multiple strains from South Tyrol (Figure 6D; Table S1). This is similar to *SRF3*, for which incompatibility alleles are found throughout Central Asia (Alcázar et al., 2010), although overall population differentiation appears to be lower in Central Asia than in South Tyrol (Figures 6D, E) (Cao et al., 2011).

Discussion

The extent to which non-additive interactions between segregating alleles affect fitness related traits in both outcrossing and selfing organisms is a central question in genetics (Corbett-Detig et al., 2013; Mackay, 2014; Phillips, 2008). We have used a new, systematically structured population of F_1 hybrids to determine the prevalence and causes of a common form of deleterious epistasis in plants, hybrid necrosis. A main finding is that interactions among immune genes are the most common cause of hybrid necrosis; this observation indicates that there are limits to the assembly of potentially favorable immune gene alleles in the same genetic background.

The crosses we investigated included parental pairs that were from the same location and sometimes closely related throughout the genome, as well as geographically and genetically distant parents. We found that genome-wide genetic differentiation, which is correlated with geographic distance in *A. thaliana* (Cao et al., 2011), is not a good predictor for hybrid incompatibility. We interpret the occurrence of incompatibilities between accessions from the same geographic region as a sign that the incompatibilities on their own do not greatly affect the frequency of the individual causal alleles in the population. The genetic architectures we uncovered include interactions between one locus and several other distinct loci (*DM2* with *DM1*, *DM3*, *DM4*, *DM5* and *SRF3*), between different pairs of alleles at the same two loci (*DM6* with *DM7*), and between different alleles at the same locus (at *DM8* and at *DM9*). This highlights that particular loci are disproportionately dangerous, and can repeatedly cause independent deleterious epistatic interactions. Another important finding is that a large fraction of the hybrid necrosis alleles map to plant NLR immune receptor loci. While we do not yet have proof that any of the specific alleles we have identified are beneficial in nature, the extreme variability of a subset of immune genes is in itself thought to be advantageous, particularly where resistance genes co-evolve with extant pathogens (Holub, 2001; Michelmore and Meyers, 1998; Yang et al., 2013). Moreover, crop breeders have actively selected hybrid necrosis genes because they confer agronomically relevant resistances (Bomblies and Weigel, 2007; Krüger et al., 2002). This specific connection to the immune system sets our study apart from intraspecific studies in other systems where the

evolutionary forces that give rise to deleterious epistasis remain largely unknown (Corbett-Detig et al., 2013).

It may not appear surprising that many hybrid necrosis genes encode NLR proteins, but two findings were unexpected: that *RPP* genes, which correspond to the major regions of the *A. thaliana* genome that encode resistance to the pathogen *Hpa* (Holub and Beynon, 1997; Nemri et al., 2010) are over-represented, and that a single locus, *DM2*/*RPP1*, is involved in over half of all hybrid necrosis cases mapped to date. Among *RPP* genes, *RPP1* appears to be the most versatile locus, with alleles conferring resistance against many different *Hpa* genotypes and mediating different necrosis phenotypes (Holub and Beynon, 1997). That *DM2/RPP1* is at the same time a frequent trigger of autoimmunity underscores the potential dangers of a rapidly evolving immune system, both with respect to new mutations at this locus, and upon outcrossing between accessions.

Because we found several interactions between different alleles at the same locus, our observations have implications not only for what has been called statistical epistasis, which is concerned with interactions between segregating polymorphisms, but also for functional epistasis, which refers to the allowed mutational paths of individual loci (Weinreich et al., 2005). Similar to *DM2*/*RPP1*, NLR genes are often arranged in tandem arrays. In a single tandem array, mutations could arise that cause deleterious interactions between proteins encoded by different members of such an array, but these would presumably be selected against, thereby limiting diversification within the array. In this context, it is of interest that the hybrid necrosis activity of the $DM2h^{\text{Bla-1}}$ allele was apparently acquired stepwise, as deduced from our experiments with domain swaps.

Perhaps the most important conclusion from our findings is that autoimmunity in hybrids might limit the assembly of superior immune alleles into a single genotype, because of the interactions between NLRs and other loci involved in immunity. We note that the self-fertilizing mating system of *A. thaliana* is not a barrier to the rapid reassortment of genetic diversity. In the native range of the species, identical multi-locus haplotypes are generally confined to individual small stands, and outcrossing rates in nature are sufficient to frequently generate new genetic combinations (Bomblies et al., 2010). It is noteworthy that we identified several accessions that carry multiple hybrid necrosis risk alleles. For example, the ICE163 accession carries both a *DM2* risk allele that is incompatible with *DM4* from TueWa1-2, and a risk allele at *DM5* that is incompatible with *DM2* from Dog-4. Similarly, hybrid necrosis alleles at both *DM2* and *DM9* are found in Bla-1, at both *DM4* and *DM7* in TueWa1-2, and at both *DM7* and an unmapped class 5 locus in TueScha-9 (Table S1). Multiple incompatibility risk alleles in the same genome would increase the chances of deleterious epistasis between immune genes upon crosses with other genotypes.

While most hybrid necrosis alleles appear to be rare, we emphasize that we have limited our analyses to cases that are associated with strong morphological defects. These cases are almost certainly only the extremes of a wider range of interactions that lead to autonomous activation of the immune system. This argument follows from several observations: First, the F_1 hybrid necrosis cases display a range of severity, with some dying without flowering and others being able to set seeds as dwarves, and one of the *DM2* cases described in the

literature is expressed only in the F_2 generation (Alcázar et al., 2009). Similarly, in our diallel among the 80 fully sequenced accessions, we have observed dozens of weakly necrotic F_1 cases, several of which showed stronger symptoms in the F_2 generation. Thus, it is likely that in addition to the interactions we have reported here there are others that cause milder immune phenotypes, but still limit growth and development in a manner that is disadvantageous in the wild. Second, expression of hybrid necrosis symptoms can be modulated by genetic background (Alcázar et al., 2009), suggesting that more complex crossing strategies than the biparental design used here may reveal additional cases of hybrid necrosis.

Epistatic interactions between components of the immune system are likely to be relevant in other kingdoms as well. Such interactions have, for example, been observed in mammals, where there is evidence for positive selection acting on specific combinations of KIR-type receptors and MHC class I ligands (Single et al., 2007). Allelic variation at these loci is also responsible for autoimmune syndromes (Trowsdale and Knight, 2013). In *A. thaliana*, it seems perhaps unlikely that the interactions between the specific hybrid necrosis risk alleles we have described are beneficial, but it is conceivable that interaction between other alleles at these loci have positive effects on immune function. This can in principle be addressed using population genomic data, but because of the extreme variability of many of these loci, current whole-genome resequencing datasets are insufficient to ask directly whether specific alleles co-occur more often than expected by chance.

An important question for the future will be the biochemical nature of the interactions between hybrid necrosis risk alleles, and how they differ from interactions between non-risk alleles. *DM2* risk alleles trigger hybrid necrosis when combined with alleles at loci that encode a broad range of biochemical functions, including at least one NLR, *DM1*, consistent with other cases of NLR proteins that act in pairs (Eitas and Dangl, 2010). Two other natural *DM2* interactors encode a kinase (*SRF3*, (Alcázar et al., 2010)) and a prolyl aminopeptidase (*DM3*, this work). In addition, a chemically induced allele at a gene encoding a cysteine synthase can combine with a natural *DM2* allele to cause necrosis (Tahir et al., 2012). Outside of *A. thaliana*, hybrid necrosis alleles encode a cysteine protease (Krüger et al., 2002), a kinase (Yamamoto et al., 2010) and a subtilisin-like protease (Chen et al., 2014). Enzyme-encoding genes are clearly enriched, but in most cases we do not know yet how they modulate the activity of NLRs.

In conclusion, we propose that the study of hybrid necrosis can provide important insights into the role of epistatic interactions, particularly between immune genes, in the evolution of genotypes with multiple resistances to diverse pathogens. That hybrid necrosis alleles can increase functional disease resistance in crop breeding programs suggests that greater immune effectiveness may be tied to autoimmune risk. Understanding the relationship between effectiveness in pathogen recognition and autoimmunity will have applications in crop breeding, where it can help to guide strategies for maximizing disease resistance while minimizing yield penalties. Finally, it will be important to investigate whether the immune system of obligatory outbreeding species is more or less constrained than that of self-compatible species, and whether it therefore produces adverse effects in progeny less or more often.

Experimental Procedures

Plant material

F_1 hybrids were grown at 16°C, under long days (16 hours of light). They were monitored for signs of autoimmunity-associated morphological defects for the first 12 weeks of growth. Afterwards, plants were transferred to 23°C, and F_2 seeds were harvested from individual plants that did not carry the sterility inducing *AP3* amiRNA transgene. Class 4 and 5 hybrids were additionally grown at 28 °C.

Genotyping and QTL analyses

A GBS approach was used for genotyping F_2 mapping populations, with *Pst*I/*Mse*I double digested tags. Sequence tags and segregating SNPs for bulk segregants were generated either on Illumina GAIIx or Illumina HiSeq 2000 (Illumina, San Diego, CA). Filtered markers were used for further QTL analyses (Table S3).

DM sequence analyses

A total of six fosmid clones each were Sanger shotgun sequenced to assemble the *DM2* locus in Bla-1 and Uk-1. Illumina reads of 87 *A. thaliana* accessions (from (Cao et al., 2011) plus Col-0, L*er*, Uk-1, Uk-3, Uk-6, Nc-1, Bla-1) and *A. lyrata* MN47 were trimmed to 36 bp in length and aligned to $DM2d^{\text{Uk-1}}$ and $DM2h^{\text{Bla-1}}$ open reading frames as reference using GenomeMapper (Schneeberger et al., 2009). One mismatch and zero gaps were allowed. Matrices were generated by assigning a value of one to each position covered by at least one read, and a value of zero to the remaining positions. Resulting profiles were clustered using complete linkage clustering with Euclidean distance.

Population genetic analyses

One-hundred-kb regions upstream or downstream of three NLR loci were extracted from a genome variant matrix (Cao et al., 2011). Only positions with allele frequency above 0.1 were retained, and ten consecutive SNPs were binned for further calculations. The ‘compute’ program, based on the ‘libsequence’ C++ library (Thornton, 2003), was used to calculate haplotype diversity.

Accession numbers

Short reads of Uk-3, Uk-6, KZ10 and Mrk-0 have been deposited in the European Nucleotide Archive under the accession number ERP005469. Sequences of the *DM2* regions from Bla-1 and Uk-1, of *DM3* from Hh-0, and of the *RPW8* region from KZ10 have been deposited in GenBank under accession numbers KJ454428, KJ45449, KJ634210 and KJ634211.

Supplementary Material

Refer to Web version on PubMed Central for supplementary material.

Acknowledgments

We thank Rubén Alcázar, Jane Parker and Maarten Koornneef for information regarding *RPP1*, Jesse Poland for GBS advice, Frank Wellmer for the *AP3* amiRNA, Eui-Hwan Chung and Jeffery Dangl for pointers on cell death assays, William Ho, Paula Sancha-Vilchez and Josip Perkovic for technical support, and Jeffery Dangl, Ya-Long Guo, Daniel Koenig, George Wang and Jun Cao for discussion. We especially thank the anonymous reviewers, who greatly helped us with the evolutionary framing of our work. This work was supported by an NIH Ruth Kirschstein NRSA (K.B.), an HFSP Long-Term Fellowship (R.A.L.), an Alexander von Humboldt Foundation Fellowship (B.A.R.), an HFSPO Grant (RGP 57/2007), a Gottfried Wilhelm Leibniz Award of the DFG and the Max Planck Society (D.W.).

References

Alcázar R, García AV, Kronholm I, de Meaux J, Koornneef M, Parker JE, Reymond M. Natural variation at Strubbelig Receptor Kinase 3 drives immune-triggered incompatibilities between *Arabidopsis thaliana* accessions. Nat Genet. 2010; 42:1135–1139. [PubMed: 21037570]

Alcázar R, Garcia AV, Parker JE, Reymond M. Incremental steps toward incompatibility revealed by *Arabidopsis* epistatic interactions modulating salicylic acid pathway activation. Proc Natl Acad Sci USA. 2009; 106:334–339. [PubMed: 19106299]

Allen RL, Bittner-Eddy PD, Grenville-Briggs LJ, Meitz JC, Rehmany AP, Rose LE, Beynon JL. Host-parasite coevolutionary conflict between *Arabidopsis* and downy mildew. Science. 2004; 306:1957–1960. [PubMed: 15591208]

Bakker EG, Toomajian C, Kreitman M, Bergelson J. A genome-wide survey of *R* gene polymorphisms in *Arabidopsis*. Plant Cell. 2006; 18:1803–1818. [PubMed: 16798885]

Bateson, V. Heredity and variation in modern lights. In: Seward, AC., editor. Darwin and Modern Science. Cambridge: Cambridge University Press; 1909. p. 85-101.

Bikard D, Patel D, Le Mette C, Giorgi V, Camilleri C, Bennett MJ, Loudet O. Divergent evolution of duplicate genes leads to genetic incompatibilities within *A. thaliana*. Science. 2009; 323:623–626. [PubMed: 19179528]

Bomblies K, Lempe J, Epple P, Warthmann N, Lanz C, Dangl JL, Weigel D. Autoimmune response as a mechanism for a Dobzhansky-Muller-type incompatibility syndrome in plants. PLoS Biol. 2007; 5:e236. [PubMed: 17803357]

Bomblies K, Weigel D. Hybrid necrosis: autoimmunity as a potential gene-flow barrier in plant species. Nat Rev Genet. 2007; 8:382–393. [PubMed: 17404584]

Bomblies K, Yant L, Laitinen RA, Kim ST, Hollister JD, Warthmann N, Fitz J, Weigel D. Local-scale patterns of genetic variability, outcrossing, and spatial structure in natural stands of *Arabidopsis thaliana*. PLoS Genet. 2010; 6:e1000890. [PubMed: 20361058]

Cao J, Schneeberger K, Ossowski S, Gunther T, Bender S, Fitz J, Koenig D, Lanz C, Stegle O, Lippert C, et al. Whole-genome sequencing of multiple *Arabidopsis thaliana* populations. Nat Genet. 2011; 43:956–963. [PubMed: 21874002]

Chen C, Chen H, Lin YS, Shen JB, Shan JX, Qi P, Shi M, Zhu MZ, Huang XH, Feng Q, et al. A two-locus interaction causes interspecific hybrid weakness in rice. Nat Commun. 2014; 5:3357. [PubMed: 24556665]

Chin DB, Arroyo-Garcia R, Ochoa OE, Kesseli RV, Lavelle DO, Michelmore RW. Recombination and spontaneous mutation at the major cluster of resistance genes in lettuce (*Lactuca sativa*). Genetics. 2001; 157:831–849. [PubMed: 11157000]

Chung EH, da Cunha L, Wu AJ, Gao Z, Cherkis K, Afzal AJ, Mackey D, Dangl JL. Specific threonine phosphorylation of a host target by two unrelated type III effectors activates a host innate immune receptor in plants. Cell Host Microbe. 2011; 9:125–136. [PubMed: 21320695]

Collier SM, Moffett P. NB-LRRs work a “bait and switch” on pathogens. Trends Plant Sci. 2009; 14:521–529. [PubMed: 19720556]

Corbett-Detig RB, Zhou J, Clark AG, Hartl DL, Ayroles JF. Genetic incompatibilities are widespread within species. Nature. 2013; 504:135–137. [PubMed: 24196712]

Coyne, JA.; Orr, HA. Speciation. Sunderland, MA: Sinauer; 2004.

Crespi B, Nosil P. Conflictual speciation: species formation via genomic conflict. Trends Ecol Evol. 2013; 28:48–57. [PubMed: 22995895]

Cutter AD. The polymorphic prelude to Bateson-Dobzhansky-Muller incompatibilities. Trends Ecol Evol. 2012; 27:209–218. [PubMed: 22154508]

Dobzhansky, T. Genetics and the Origin of Species. New York: Columbia University Press; 1937.

Eitas TK, Dangl JL. NB-LRR proteins: pairs, pieces, perception, partners, and pathways. Curr Opin Plant Biol. 2010; 13:472–477. [PubMed: 20483655]

Elshire RJ, Glaubitz JC, Sun Q, Poland JA, Kawamoto K, Buckler ES, Mitchell SE. A robust, simple genotyping-by-sequencing (GBS) approach for high diversity species. PLoS ONE. 2011; 6:e19379. [PubMed: 21573248]

Harris CJ, Slootweg EJ, Goverse A, Baulcombe DC. Stepwise artificial evolution of a plant disease resistance gene. Proc Natl Acad Sci USA. 2013; 110:21189–21194. [PubMed: 24324167]

Holub EB. The arms race is ancient history in *Arabidopsis*, the wildflower. Nat Rev Genet. 2001; 2:516–527. [PubMed: 11433358]

Holub EB, Beynon JL. Symbiology of mouse-ear cress (*Arabidopsis thaliana*) and oomycetes. Adv Bot Res. 1997; 24:227–273.

Hou J, Friedrich A, de Montigny J, Schacherer J. Chromosomal rearrangements as a major mechanism in the onset of reproductive isolation in *Saccharomyces cerevisiae*. Curr Biol. 2014; 24:1153–1159. [PubMed: 24814147]

Jacob F, Vernaldi S, Maekawa T. Evolution and Conservation of Plant NLR Functions. Frontiers in immunology. 2013; 4:297. [PubMed: 24093022]

Jeuken MJ, Zhang NW, McHale LK, Pelgrom K, den Boer E, Lindhout P, Michelmore RW, Visser RG, Niks RE. *RIN4* causes hybrid necrosis and race-specific resistance in an interspecific lettuce hybrid. Plant Cell. 2009; 21:3368–3378. [PubMed: 19855048]

Krasileva KV, Dahlbeck D, Staskawicz BJ. Activation of an *Arabidopsis* resistance protein is specified by the in planta association of its leucine-rich repeat domain with the cognate oomycete effector. Plant Cell. 2010; 22:2444–2458. [PubMed: 20601497]

Krüger J, Thomas CM, Golstein C, Dixon MS, Smoker M, Tang S, Mulder L, Jones JD. A tomato cysteine protease required for Cf-2-dependent disease resistance and suppression of autonecrosis. Science. 2002; 296:744–747. [PubMed: 11976458]

Kuang H, Woo SS, Meyers BC, Nevo E, Michelmore RW. Multiple genetic processes result in heterogeneous rates of evolution within the major cluster disease resistance genes in lettuce. Plant Cell. 2004; 16:2870–2894. [PubMed: 15494555]

Lachance J, True JR. X-autosome incompatibilities in *Drosophila melanogaster*: tests of Haldane's rule and geographic patterns within species. Evolution. 2010; 64:3035–3046. [PubMed: 20455929]

Lu H, Rate DN, Song JT, Greenberg JT. ACD6, a novel ankyrin protein, is a regulator and an effector of salicylic acid signaling in the *Arabidopsis* defense response. Plant Cell. 2003; 15:2408–2420. [PubMed: 14507999]

Mackay TF. Epistasis and quantitative traits: using model organisms to study gene-gene interactions. Nat Rev Genet. 2014; 15:22–33. [PubMed: 24296533]

Maheshwari S, Barbash DA. The genetics of hybrid incompatibilities. Annu Rev Genet. 2011; 45:331–355. [PubMed: 21910629]

Michelmore RW, Meyers BC. Clusters of resistance genes in plants evolve by divergent selection and a birth-and-death process. Genome Res. 1998; 8:1113–1130. [PubMed: 9847076]

Muller HJ. Isolating mechanisms, evolution and temperature. Biol Symp. 1942; 6:71–125.

Nemri A, Atwell S, Tarone AM, Huang YS, Zhao K, Studholme DJ, Nordborg M, Jones JD. Genome-wide survey of *Arabidopsis* natural variation in downy mildew resistance using combined association and linkage mapping. Proc Natl Acad Sci USA. 2010; 107:10302–10307. [PubMed: 20479233]

Phillips PC. Epistasis–the essential role of gene interactions in the structure and evolution of genetic systems. Nat Rev Genet. 2008; 9:855–867. [PubMed: 18852697]

Phillips PC, Johnson NA. The population genetics of synthetic lethals. Genetics. 1998; 150:449–458. [PubMed: 9725860]

Poland JA, Brown PJ, Sorrells ME, Jannink JL. Development of high-density genetic maps for barley and wheat using a novel two-enzyme genotyping-by-sequencing approach. PLoS ONE. 2012; 7:e32253. [PubMed: 22389690]

Presgraves DC. The molecular evolutionary basis of species formation. Nat Rev Genet. 2010; 11:175–180. [PubMed: 20051985]

Quintana-Murci L, Clark AG. Population genetic tools for dissecting innate immunity in humans. Nat Rev Immunol. 2013; 13:280–293. [PubMed: 23470320]

Rieseberg LH, Blackman BK. Speciation genes in plants. Ann Bot. 2010; 106:439–455. [PubMed: 20576737]

Sackton TB, Lazzaro BP, Schlenke TA, Evans JD, Hultmark D, Clark AG. Dynamic evolution of the innate immune system in *Drosophila*. Nat Genet. 2007; 39:1461–1468. [PubMed: 17987029]

Schneeberger K, Ossowski S, Lanz C, Juul T, Petersen AH, Nielsen KL, Jørgensen JE, Weigel D, Andersen SU. SHOREmap: simultaneous mapping and mutation identification by deep sequencing. Nat Methods. 2009; 6:550–551. [PubMed: 19644454]

Segretin ME, Pais M, Franceschetti M, Chaparro-Garcia A, Bos JI, Banfield MJ, Kamoun S. Single amino acid mutations in the potato immune receptor R3a expand response to Phytophthora effectors. Molecular plant-microbe interactions: MPMI. 2014

Seidel HS, Rockman MV, Kruglyak L. Widespread genetic incompatibility in C. elegans maintained by balancing selection. Science. 2008; 319:589–594. [PubMed: 18187622]

Single RM, Martin MP, Gao X, Meyer D, Yeager M, Kidd JR, Kidd KK, Carrington M. Global diversity and evidence for coevolution of *KIR* and *HLA*. Nat Genet. 2007; 39:1114–1119. [PubMed: 17694058]

Steinbrenner AD, Goritschnig S, Krasileva KV, Schreiber KJ, Staskawicz BJ. Effector recognition and activation of the *Arabidopsis thaliana* NLR innate immune receptors. Cold Spring Harb Symp Quant Biol. 2012; 77:249–257. [PubMed: 23174767]

Tahir J, Watanabe M, Jing HC, Hunter DA, Tohge T, Nunes-Nesi A, Brotman Y, Fernie AR, Hoefgen R, Dijkwel PP. Activation of R-mediated innate immunity and disease susceptibility is affected by mutations in a cytosolic O-acetylserine (thiol) lyase in *Arabidopsis*. Plant J. 2012

Thornton K. Libsequence: a C++ class library for evolutionary genetic analysis. Bioinformatics. 2003; 19:2325–2327. [PubMed: 14630667]

Todesco M, Balasubramanian S, Hu TT, Traw MB, Horton M, Epple P, Kuhns C, Sureshkumar S, Schwartz C, Lanz C, et al. Natural allelic variation underlying a major fitness tradeoff in *Arabidopsis thaliana*. Nature. 2010; 465:632–636. [PubMed: 20520716]

Todesco M, Kim ST, Chae E, Bomblies K, Zaidem M, Smith LM, Weigel D, Laitinen RA. Activation of the *Arabidopsis thaliana* immune system by combinations of common *ACD6* alleles. PLoS Genet. 2014; 10:e1004459. [PubMed: 25010663]

Trowsdale J, Knight JC. Major histocompatibility complex genomics and human disease. Annu Rev Genomics Hum Genet. 2013; 14:301–323. [PubMed: 23875801]

Vilches C, Parham P. KIR: diverse, rapidly evolving receptors of innate and adaptive immunity. Annu Rev Immunol. 2002; 20:217–251. [PubMed: 11861603]

Weinreich DM, Watson RA, Chao L. Perspective: Sign epistasis and genetic constraint on evolutionary trajectories. Evolution. 2005; 59:1165–1174. [PubMed: 16050094]

Wuest SE, O'Maoileidigh DS, Rae L, Kwasniewska K, Raganelli A, Hanczaryk K, Lohan AJ, Loftus B, Graciet E, Wellmer F. Molecular basis for the specification of floral organs by APETALA3 and PISTILLATA. Proc Natl Acad Sci USA. 2012; 109:13452–13457. [PubMed: 22847437]

Xiao S, Ellwood S, Calis O, Patrick E, Li T, Coleman M, Turner JG. Broad-spectrum mildew resistance in *Arabidopsis thaliana* mediated by *RPW8*. Science. 2001; 291:118–120. [PubMed: 11141561]

Yamamoto E, Takashi T, Morinaka Y, Lin S, Wu J, Matsumoto T, Kitano H, Matsuoka M, Ashikari M. Gain of deleterious function causes an autoimmune response and Bateson–Dobzhansky–Muller incompatibility in rice. Mol Genet Genomics. 2010; 283:305–315. [PubMed: 20140455]

Yang S, Li J, Zhang X, Zhang Q, Huang J, Chen JQ, Hartl DL, Tian D. Rapidly evolving *R* genes in diverse grass species confer resistance to rice blast disease. Proc Natl Acad Sci USA. 2013; 110:18572–18577. [PubMed: 24145399]

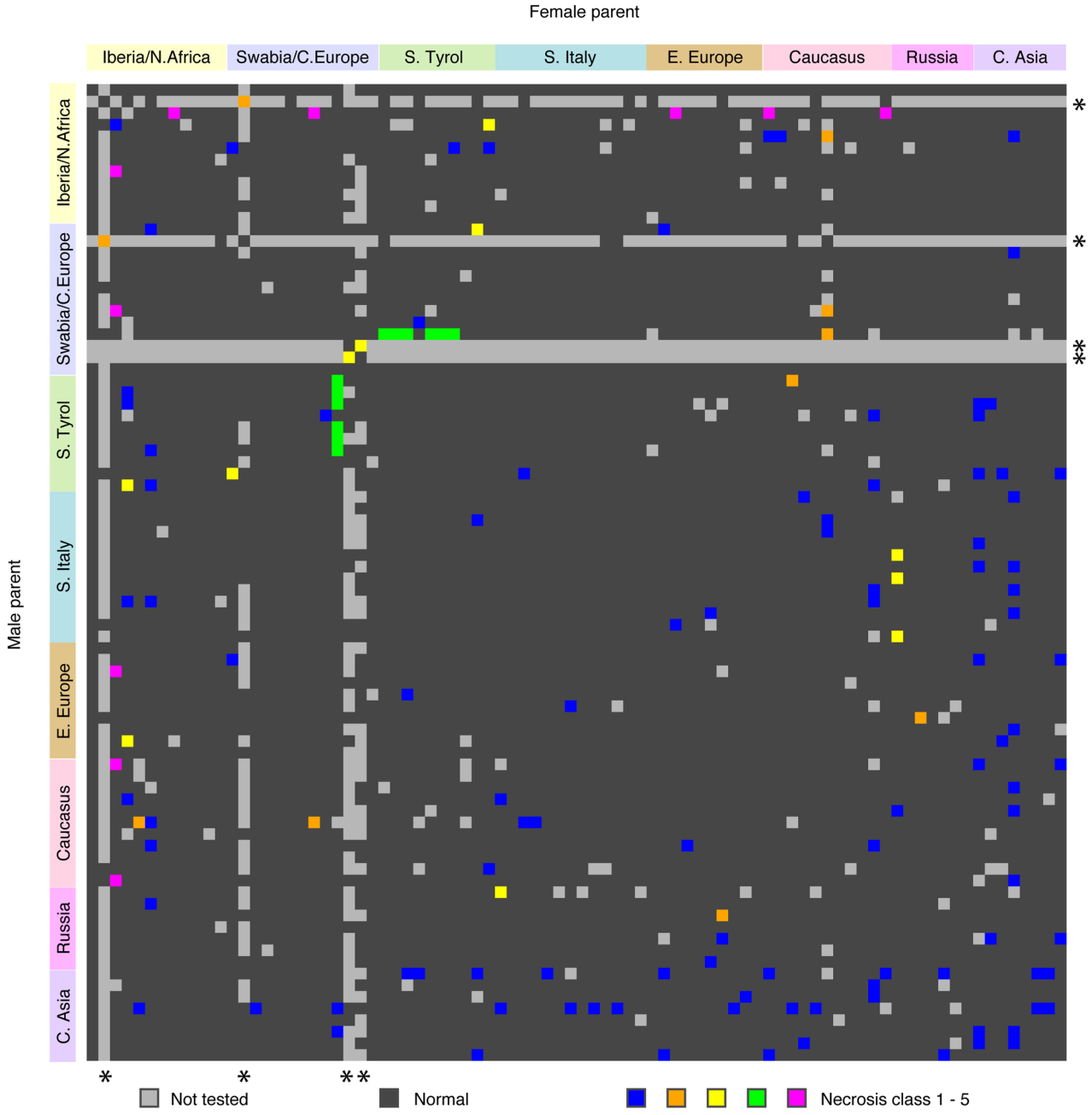

Figure 1. Crosses for Detection of Hybrid Incompatibilities

Accessions are color coded by region of origin. Accessions that are not part of the 80 accessions from (Cao et al., 2011) are marked with asterisks.

See also Figure S1 and Table S1.

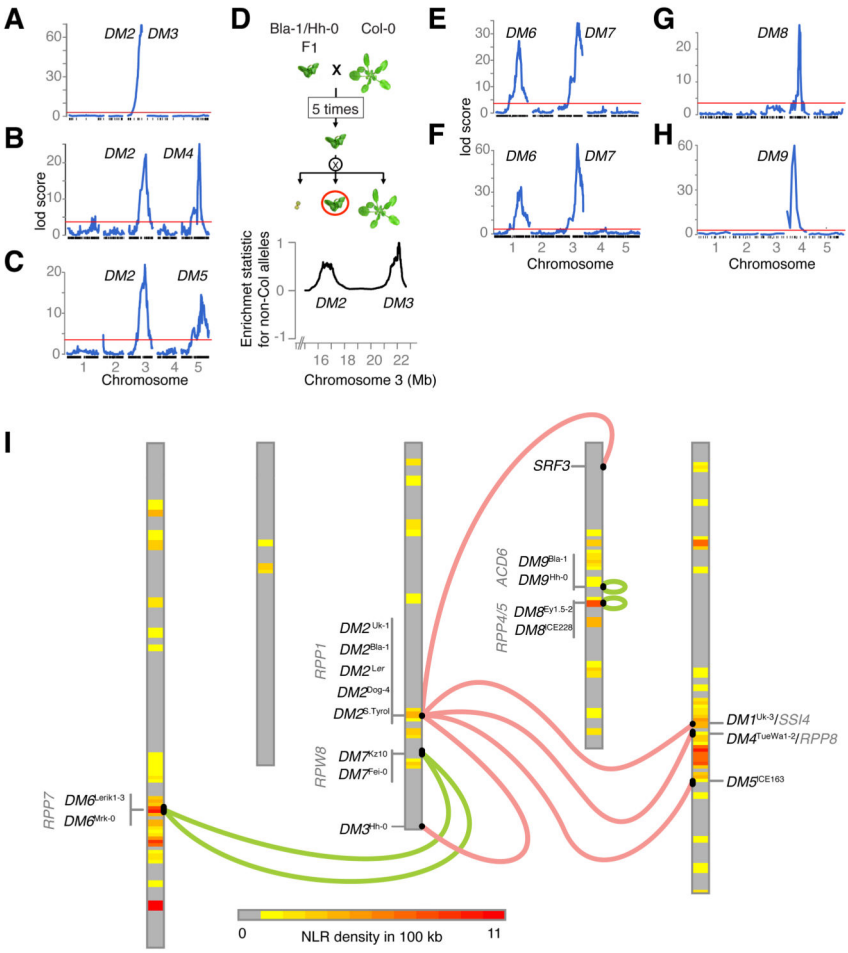

Figure 2. Linkage Mapping of Seven Hybrid Incompatibilities

Hybrid necrosis QTL maps in (A) Bla-1/Hh-0 (leaf twisting), (B) TueWa1-2/ICE163, (C) Dog-4/ICE163, (E) Fei-0/Lerik1-3, (F) KZ10/Mrk-0, (G) Ey1.5-2/ICE228, and (H) Bla-1/Hh-0 (late-onset lesioning). Red lines mark significance threshold (p=0.05, 1,000 permutations); vertical marks along the X-axes indicate marker positions.

(D) Scheme for Illumina sequencing of bulk segregants to delineate *DM2* and *DM3*.

(I) Genomic location of *DM* alleles compared to NLR gene density (1 Mb windows) on the five chromosomes of the reference strain Col-0. *SRF3*, $DM2^{Ler}$ and *DM1/SSI4* have been reported before (Alcázar et al., 2010; Alcázar et al., 2009; Bomblies et al., 2007). *DM2/RPP1* interactions in red, others in green.

See also Figure S2, Tables S2, S3 and S4.

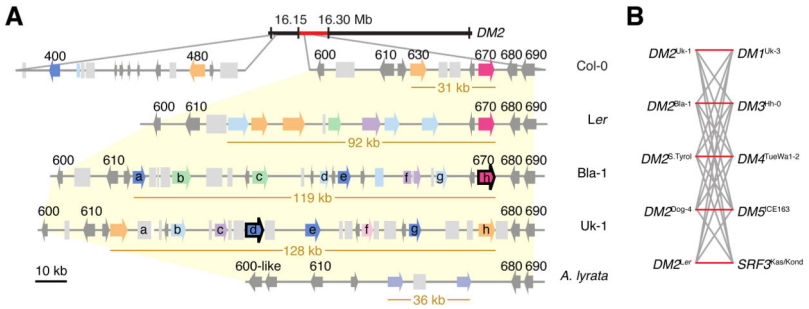

Figure 3. The *DM2* Cluster in *Arabidopsis*

(A) *DM2* clusters in four *A. thaliana* accessions and in *A. lyrata* MN47. The mapping interval for *DM2* in Bla-1 is indicated in red. Genes are indicated with colored arrows, pseudogenes with colored boxes and transposons with light grey boxes. Non-NLR genes are in dark grey. NLR genes are colored according to their phylogenetic history (see Figure S4), with unresolved relationships indicated in light blue. Numbers above arrows indicate the last three digits of At3g44XXX and are given only when there are homologs in the reference genome. The two incompatibility genes are outlined in black. The $DM2^{Ler}$ cluster was re-annotated based on GenBank FJ446580.1. The sizes in kb refer to the core *DM2* clusters, defined as the coding regions of all NLRs (colored arrows) in a cluster.

(B) Test crosses between *DM2* carriers and interacting allele carriers. Red and grey lines indicate incompatible and compatible interactions, respectively.

See also Figure S3.

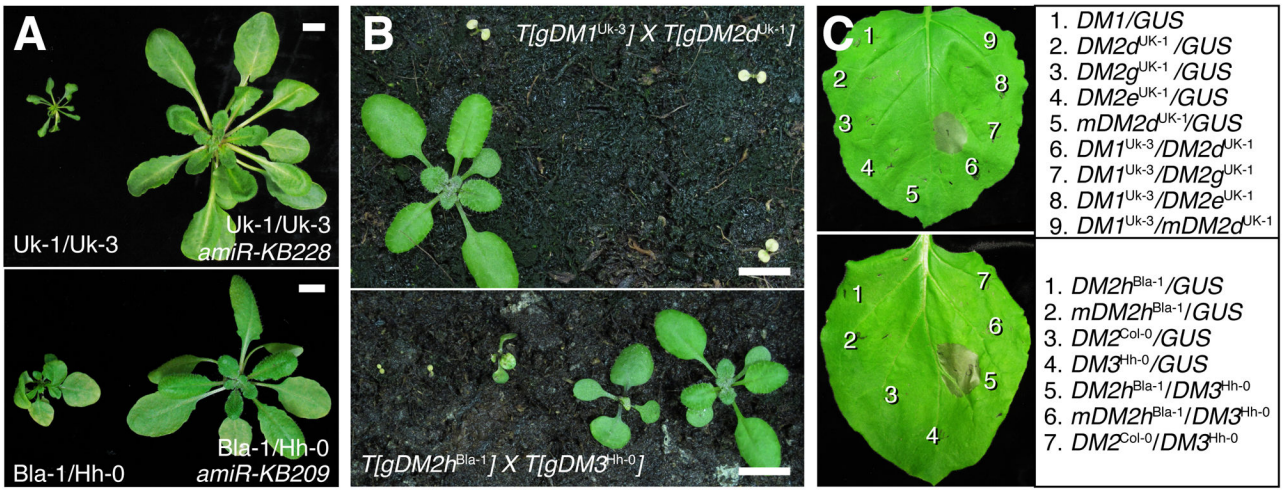

Figure 4. Identification of *DM2d*$^{\text{Uk-1}}$ and *DM2h*$^{\text{Bla-1}}$ as Hybrid Necrosis Genes

(A) *Arabidopsis thaliana* F_1 hybrids and rescued siblings expressing amiRNAs at 16 °C.

(B) Reconstitution of incompatibilities in Col-0, with transgenic F_1 hybrids at 16°C. Transgenic effects were often stronger than F_1 hybrid phenotypes.

(C) HR-like cell death in *N. benthamiana* induced by co-expression of *A. thaliana* DM proteins at 23°C. mDM2 indicates P-loop mutant versions (GIGKTT to GIAATT), which should not be able to bind and hydrolyze ATP (Chung et al., 2011).

Scale bars in (A) and (B) represent 1 cm.

See also Figure S4.

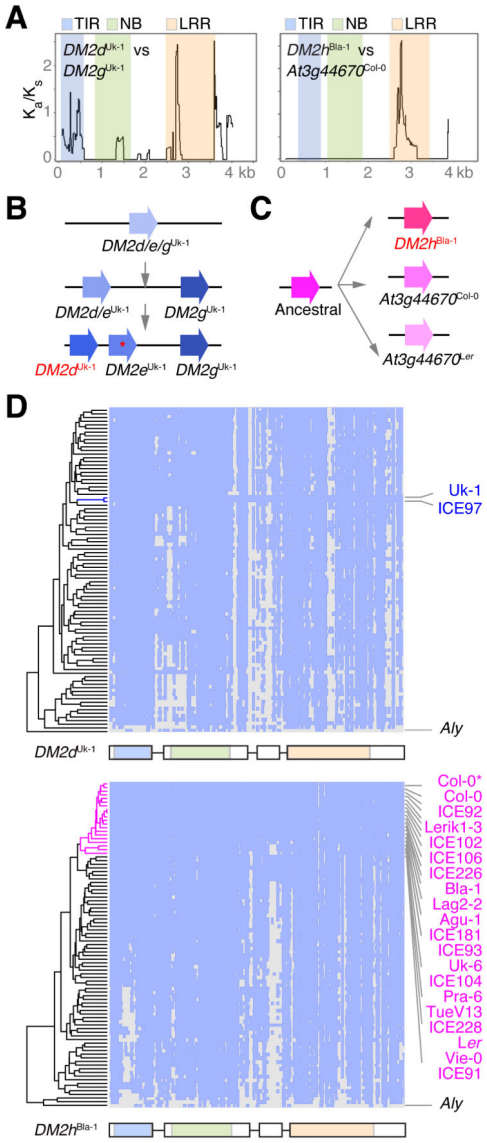

Figure 5. Origin and Variation of *DM2* Hybrid Necrosis Genes

(A) K_a/K_s ratios of closely related *DM2* genes (window length 150 bp, step size 9 bp).

(B) Most parsimonious path for evolution of *DM2d*$^{Uk-1}$ paralogs.

(C) Most parsimonious path for evolution of *DM2h*$^{Bla-1}$ orthologs.

(D) *DM2d*$^{Uk-1}$- and *DM2h*$^{Bla-1}$-type profiling using Illumina reads from accessions with one mismatch. Grey indicates uncovered regions. Accessions carrying a *DM2h*-type are labeled in magenta.

See also Figure S5, Tables S5 and S6.

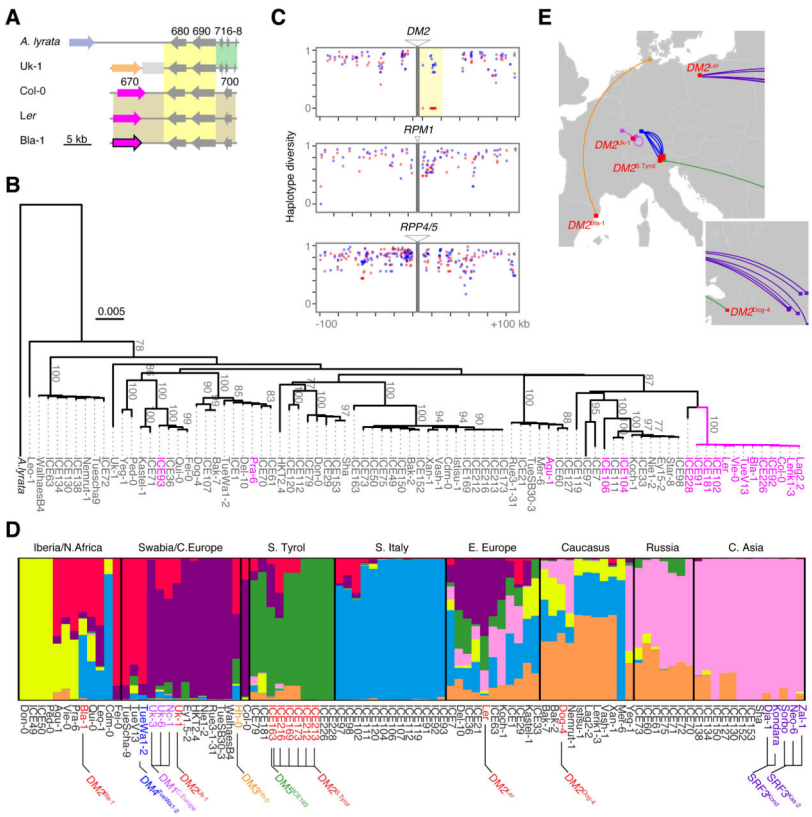

Figure 6. Haplotype Sharing Around *DM2h* and Geographic Distribution of *DM2* alleles

(A) Syntenic overview of the region beyond the *DM2* clusters in *A. thaliana* accessions and in *A. lyrata* MN47. See Fig. 3A legend for color and number code.

(B) Phylogeny of 8-kb conserved sequences spanning At3g44680 and At3g44690 (yellow shade in panel A). *DM2h*-type carriers are magenta, non-carriers grey. Bootstrap values over 70% are indicated.

(C) Haplotype diversity based on groups of 10 adjacent SNPs in the regions flanking NLR loci *DM2*, *RPM1* and *RPP4/5*. Twelve *DM2h*-type carriers in red and 12 non-carriers in blue.

(D) STRUCTURE analysis ($k = 7$) of hybrid necrosis risk allele carriers together with a selection of global accessions. At the bottom, accessions carrying different *DM2* hybrid necrosis alleles in red, and those carrying *DM2* interacting alleles in other colors. These colors are unrelated to the ones used to identify membership in STRUCTURE clusters on top.

(E) Carriers of *DM2* hybrid necrosis alleles in red, carriers of interacting alleles in other colors. *DM2/SRF3* interactions are from (Alcázar et al., 2010).

See also Figure S6.

Table 1

Candidate Genes for Hybrid Necrosis

Cross	Class*	Locus A	Evidence†	Locus B	Evidence†
Uk-1/Uk-3	3	*DM2* (*RPP1*)	Genomic/amiRNA	*DM1* (*SSI4*)	Genomic/amiRNA††
Bla-1/Hh-0 F_3[a]	2	*DM2* (*RPP1*)	Genomic/amiRNA	*DM3* (At3g61540)	Genomic/MIGS
Bla-1/Hh-0 F_2[b]	2	*DM9* (*ACD6*)	Genomic/amiRNA§	*DM9* (*ACD6*)	Genomic/amiRNA§
TueWa1-2/ICE163	4	*DM2* (*RPP1*)	Map only	*DM4 (RPP8)*	Map only
Dog-4/ICE163	2	*DM2* (*RPP1*)	Map only	*DM5*	Map only
KZ10/Mrk-0	3	*DM6* (*RPP7*)	Map only	*DM7* (*RPW8*)	Genomic
Fei-0/Lerik1-3	2	*DM6* (*RPP7*)	amiRNA	*DM7* (*RPW8*)	Map only
Ey1.5-2/ICE228	3	*DM8* (*RPP4/5*)	amiRNA	*DM8* (*RPP4/5*)	amiRNA

*Classes 1 to 3 as described (Bomblies et al., 2007). Class 4 hybrids arrest as seedlings with only cotyledons and severe necrosis at 16°C, which were recovered at 28°C to set seeds.

†'Genomic' refers to genomic fragment reproducing hybrid necrosis in transgenic plants.

††Described previously (Bomblies et al., 2007).

§Described in detail elsewhere (Todesco et al., 2014).